New Journal of Physics
The open–access journal for physics

Probing orbital order with soft x-rays: the case of the manganites

Stuart B Wilkins[1,2,6], Thomas A W Beale[3], Peter D Hatton[3], John A Purton[4], Peter Bencok[2], D Prabhakaran[5] and Andrew T Boothroyd[5]

[1] European Commission, Joint Research Center, Institute for Transuranium Elements, Hermann von Helmholtz-Platz 1, 76344 Eggenstein-Leopoldshafen, Germany
[2] European Synchrotron Radiation Facility, 38043 Grenoble Cedex, France
[3] Department of Physics, University of Durham, Rochester Building, South Road, Durham DH1 3LE, UK
[4] SRS, Daresbury Laboratory, Warrington, Cheshire WA4 4AD, UK
[5] Department of Physics, University of Oxford, Clarendon Laboratory, Parks Road, Oxford OX1 3PU, UK
E-mail: wilkins@esrf.fr

New Journal of Physics **7** (2005) 80
Received 20 December 2004
Published 15 March 2005
Online at http://www.njp.org/
doi:10.1088/1367-2630/7/1/080

Abstract. We have investigated the orbital and magnetic correlations of the manganese sub-lattice in the archetypical half-doped manganite $La_{0.5}Sr_{1.5}MnO_4$ using the enhanced sensitivity of resonant soft x-ray diffraction at the Mn L edges. We have separately measured the energy dependence of the scattered intensity from both the $(\frac{1}{4}, \frac{1}{4}, 0)$ and $(\frac{1}{4}, \frac{1}{4}, \frac{1}{2})$ reflections indicative of the long-range correlations of orbital and magnetic order respectively. Measurements of the integrated intensity of the different features in the resonant energy spectrum show the different origins of the orbital correlations and their variation with temperature. The results also give evidence for a strong coupling between the orbital and spin degrees of freedom.

[6] Author to whom any correspondence should be addressed.

PII: S1367-2630(05)91917-4

Contents

1. Introduction

Orbital ordering, which involves correlations between the spatial distribution of the outermost valence electrons, have long been considered a vital ingredient in the structural and physical properties of strongly correlated electron systems such as transition metal oxides. The competition and cooperation between the charge, orbital, and spin degrees of freedom of the electron manifests itself in unusual properties, such as high-temperature superconductivity, colossal magnetoresistance and magnetostructural transitions [1]. In particular, charge and orbital ordering of half-doped manganites has attracted much attention and controversy [2]–[6].

In this paper, we describe direct observations of the magnetic and orbital reflections in single crystals of $La_{0.5}Sr_{1.5}MnO_4$. This system is composed of MnO_2 planes separated by a cubic (LaSr)O packing layer (figure 1). In $La_{0.5}Sr_{1.5}MnO_4$ the Mn sites at room temperature are all crystallographically equivalent with an average valency of +3.5. This material displays a phase transition at ∼240 K below which it is believed that charge disproportionation of the Mn ions occurs, creating two inequivalent sites identified as Mn^{3+} and Mn^{4+} [7, 8]. The strong Hund's rule coupling and the large cubic (O_h) component of the crystal field implies that the Mn^{3+} $3d^4$ site has three electrons in the $t_{2g\uparrow}$ level and one electron in the two-fold degenerate $e_{g\uparrow}$ level. The degeneracy of the e_g level can be lifted by cooperative Jahn–Teller distortions of the MnO_6 octahedra reducing the symmetry to D_{4h}. Cooperative Jahn–Teller distortions of the MnO_6 octahedra could provide the origin of orbital ordering in the manganites due to occupation of the $3d_{3x^2-y^2}$ orbitals along the elongation direction. An alternative description as to how the orbital ordering may occur was provided by Goodenough [9]. Further cooling below $T_N \sim 120$ K results in long-range antiferromagnetic ordering of both Mn^{4+} and Mn^{3+} ions into a CE type structure (figure 2) [10]. This was intuitively predicted by Goodenough [9] who also predicted that magnetic moment arrangements would occur via orbital ordering in the higher-temperature phase. Thus the alternative model highlights orbital order correlations caused by antiferromagnetic ordering. Until very recently, such questions remained unanswered since a direct observation of orbital ordering remained elusive.

X-ray diffraction is generally sensitive to the isotropic electron density distribution. However, by tuning the photon energy to an absorption edge, enhanced sensitivity to the valence states is obtained [11, 12]. Resonant x-ray scattering (RXS) involves virtual excitations from core to valence states; core electrons are excited to empty states, and x-rays are subsequently re-emitted

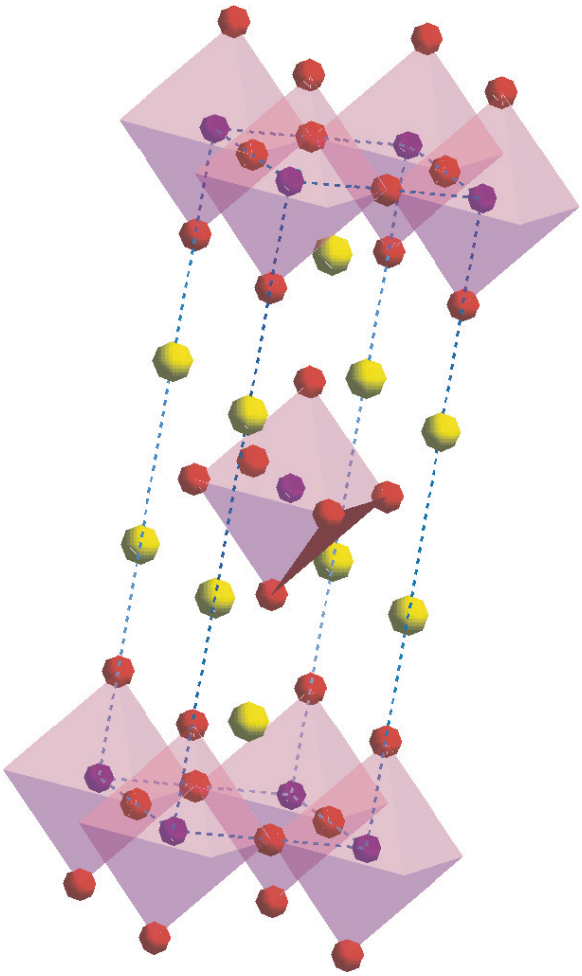

Figure 1. Crystal structure of $La_{0.5}Sr_{1.5}MnO_4$, pink octahedra represent the MnO_6 octahedra.

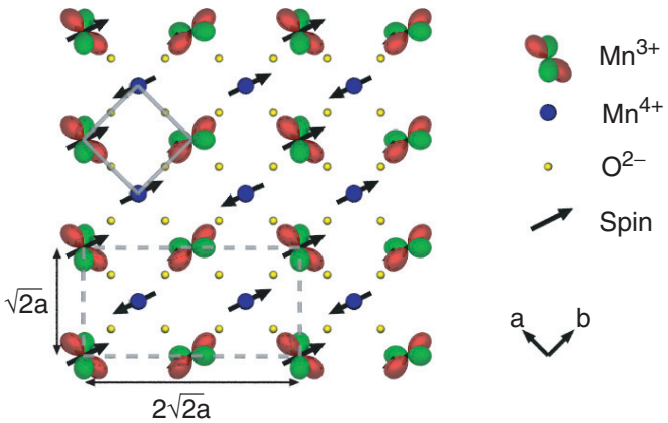

Figure 2. Schematic representation within the *ab* plane of the charge, spin and orbital ordering as predicted by Goodenough. The I4/mmm charge unit cell is shown by the solid line and the orbital ordered unit cell by the dashed line.

by their recombination [13, 14]. These processes lead to anomalous tensor components in the atomic scattering factors and hence, scattering at positions forbidden by the crystallographic space group. Such scattering can be caused by long-range ordering of magnetic moments, electronic orbital occupancy or aspherical electron density. RXS studies of $La_{0.5}Sr_{1.5}MnO_4$ were first attempted at the manganese K edge, where resonant diffraction of an orbital ordering reflection displayed a significant increase near the absorption edge and a dependence on the azimuthal angle [15]. However, the Mn K edge resonance involves virtual excitations from $1s \leftrightarrow 4p$ bands and is thus generally insensitive to orbital ordering of the 3d states. Theoretical studies proposed that the observed sensitivity is largely due to Jahn–Teller distortions, 4p band structure effects and 3d–4p Coulomb interactions [16]–[22]. However, experiments performed at the L-edges directly probe the 3d states. Resonant soft x-ray diffraction at the Mn L edges was first reported by Wilkins *et al* [23] and also the first direct observations of orbital ordering using soft x-rays in $La_{0.5}Sr_{1.5}MnO_4$ [24]. Aided by published theoretical predictions [25], they reported energy resonances at the Mn L_{III} and L_{II} edges showing that the orbital ordering was caused by a mixture of both cooperative Jahn–Teller distortions and direct Goodenough orbital correlations. These results, analysis and conclusions were later independently verified by another group [26].

The Goodenough model predicts a strong coupling between the orbital and magnetic correlations within the Mn^{3+} sub-lattice. At $T_{N(c)} = 120$ K, the antiferromagnetic order becomes fully three-dimensional. In this paper, we report high-energy resolution measurements using soft x-ray resonant diffraction on $La_{0.5}Sr_{1.5}MnO_4$ at the Mn L_{III} and L_{II} edges for both the orbital order $(\frac{1}{4}, \frac{1}{4}, 0)$ and the magnetic order $(\frac{1}{4}, \frac{1}{4}, \frac{1}{2})$ reflections. Our results allow the first direct comparison between orbital and magnetic correlations. Temperature-dependant measurements of the intensity of different features in the energy spectra show large variations, with major changes at T_N. These results demonstrate the strong interaction between orbital and spin degrees of freedom, which we believe to be a general property of many manganites and other 3d transition metal compounds.

2. Experimental details

The experiments were performed at beamline 5U1 at the SRS, Daresbury, UK and beamline ID08 at the European Synchrotron Radiation Facility, France. Single crystals of $La_{0.5}Sr_{1.5}MnO_4$ with dimensions $10 \times 3 \times 3$ mm were grown at the University of Oxford using the floating zone method. The samples were pre-aligned using a rotating anode lab x-ray source, and then cut with the [110] and [112] directions surface normal for observing the orbital and magnetic peaks respectively.

At beamline 5U1, an undulator produces soft x-rays in the range 100–1000 eV with a flux at 640 eV of approximately 1×10^{11} photons s^{-1}. The light is focused on to a plane grating as a monochromator and then refocused twice by a spherical and ellipsoidal mirror before entering the diffractometer chamber. The resulting beamsize on the sample was 0.5 mm (in the vertical) by 3 mm (horizontal). The energy resolution (ΔE) was $\approx$0.1 eV for recording the energy spectra, but was opened to $\approx$1 eV for the temperature-dependence measurements to obtain more flux. At ID08, two APPLE type undulators produce soft x-rays in the region 400–1500 eV. The light is made monochromatic by means of a spherical grating monochromator in the *dragon* configuration and post-focusing optics result in a beamsize of 50 μm (vertical) by 1 mm (horizontal). The flux incident on the sample was 10^{12} photons s^{-1} with an energy resolution of $\Delta E \approx 0.2$ eV.

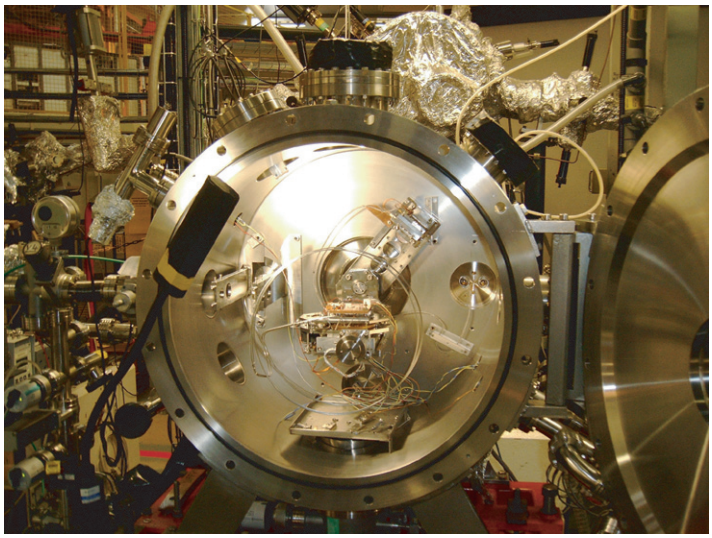

Figure 3. The in-vacuum diffraction chamber on the 5U.1 beamline at Daresbury, UK. The x-rays enter from the left, through a set of slits, and then scatter off the sample in the centre of the chamber, mounted on a liquid-nitrogen-cooled Cu stage, and are then detected by a photodiode mounted on the 2θ arm (shown here at $\sim 45^{\circ}$).

Because of the very high absorption of soft x-rays, even by air, the experiments were performed inside an in-vacuum diffractometer (figure 3) at the end of a windowless beamline. The vacuum chambers were evacuated to 10^{-7} bar during the experiments. In addition to this difficultly, the low-penetration depth of the x-rays in the sample means that the technique is relatively surface sensitive. Consequently, after aligning and cutting, the samples were polished with 0.1 μm diamond paste.

The samples were mounted on Cu pucks, which were cooled by liquid cryogens. The 5U.1 beamline is equipped with liquid nitrogen cooling, and is capable of reaching 80 K. The ID08 beamline uses liquid helium as a cryogen, and could reach temperatures down to 63 K.

3. Results and discussion

Figure 2 shows the generally accepted ground state displaying charge, spin and orbital ordering in the basal MnO_2 planes. The high temperature I4/mmm unit cell is shown by the solid line ($a = b = 3.864$ Å and $c = 12.40$ Å). Orbital and magnetic ordering reflections appear at wavevectors of $(\frac{1}{4}, \frac{1}{4}, 0)$ and $(\frac{1}{4}, \frac{1}{4}, \frac{1}{2})$ respectively. Both reflections were found to have Lorentzian-squared line shape. The top panel of figure 4 shows an energy scan at constant wavevector of 63 K through the $(\frac{1}{4}, \frac{1}{4}, 0)$ orbital order peak. The lower panel of figure 4 shows the energy scan through the antiferromagnetic $(\frac{1}{4}, \frac{1}{4}, \frac{1}{2})$ reflection at 63 K. The intensity of the scattering at the magnetic, $(\frac{1}{4}, \frac{1}{4}, \frac{1}{2})$, reflection was considerably more intense than that of the orbital, $(\frac{1}{4}, \frac{1}{4}, 0)$, reflection. In addition, the spectral weight is far more concentrated at the Mn L_{III} edge in the case of the magnetic order. In contrast to neutron measurements [8], we observed no diffuse two-dimensional scattering above T_N. This is most likely due to the normally higher wavevector resolution with x-ray measurements as compared to neutron techniques.

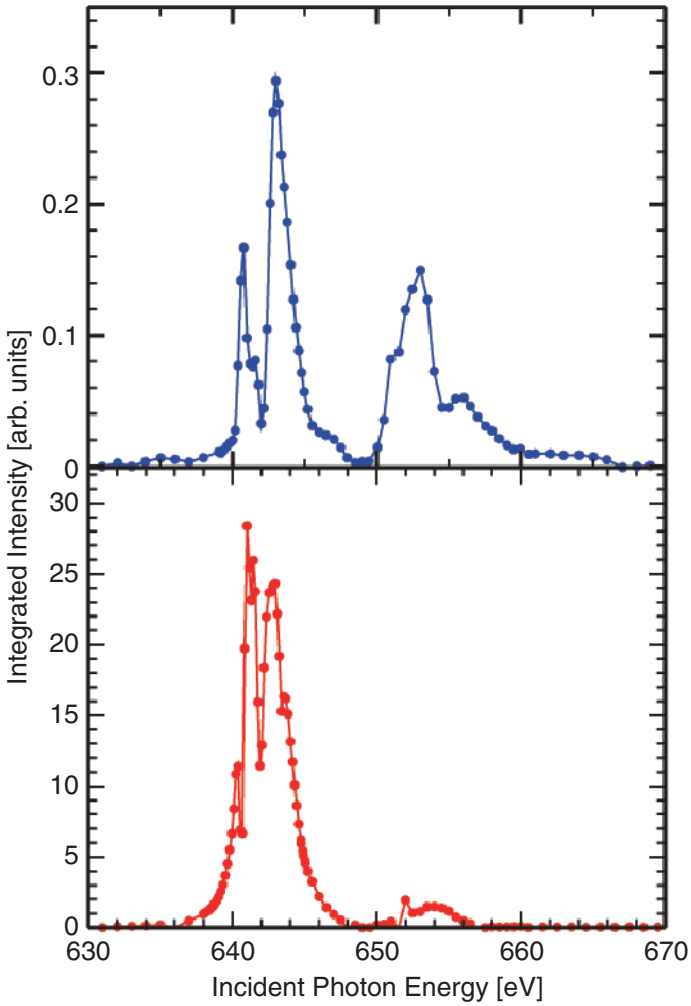

Figure 4. Energy dependence of (a) the $(\frac{1}{4}, \frac{1}{4}, 0)$ peak and (b) the $(\frac{1}{4}, \frac{1}{4}, \frac{1}{2})$ recorded over the Mn L_{III} and L_{II} edges at constant wavevector.

3.1. Azimuthal dependence

This is an important technique to establish the correct origin of the resonant scattering observed; indeed in 5f orbitally ordered systems such as NpO_2 it was vital for the correct assignment of the type of orbital order [28]. By rotating the sample around the scattering vector, it is possible to get an indication of the nature of the anisotropic components of the structure. By looking at a purely anisotropic superlattice peak (such as the $(\frac{1}{4}, \frac{1}{4}, 0)$ peak), it is possible to measure directly the anisotropy of, in this case, the alignment of the orbital ordering. Figure 5 shows the experimental data taken at ID08 compared to a simulation predicted using the anisotropy of the tensor of susceptibility. The solid curve shows a dependence given by the following equation

$$I(\theta, \psi) \propto \cos^2 \theta_B \cos^2 \Psi \cdot I_{res}^{OO} \tag{1}$$

where θ_B is the Bragg angle of the reflection and ψ is the azimuthal angle. The range of this azimuthal dependence is limited to $<180^\circ$ by the diffractometer. Azimuthal dependences are

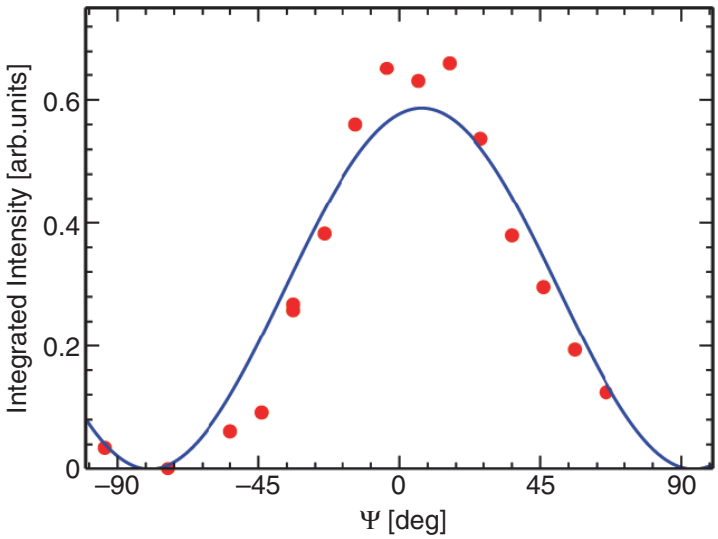

Figure 5. Dependence on the integrated intensity as a function of azimuthal angle Ψ for the $(\frac{1}{4}, \frac{1}{4}, 0)$ superlattice reflection (circles). The solid line is a simulation of the azimuthal dependence for the proposed orbital order. The fitting errors are smaller than the symbol size. This figure is reproduced from Wilkins *et al* [27].

currently very hard to measure using soft x-ray diffraction; however instrument developments are making this important technique more viable in the future.

3.2. Temperature dependence

By controlling the temperature of the sample, we are able to measure the temperature dependence of the superlattice peaks. The integrated intensity of the magnetic $(\frac{1}{4}, \frac{1}{4}, \frac{1}{2})$ reflection at an energy of 642 eV is shown in the lower panel of figure 6. This shows that the reflection is not observed, as expected, above T_N. Below T_N, it increases in intensity and continues to increase in intensity as the temperature was lowered towards the base temperature. The solid line in the lower panel of figure 6 is a fit to a power law. Figure 6 (upper panel) shows the integrated intensity of features at 643 and 653 eV in the $(\frac{1}{4}, \frac{1}{4}, 0)$ orbital reflection as a function of temperature. As discussed in our earlier papers [24, 25], scattering at the Mn L_{III} edge (∼643 eV) is primarily associated with cooperative Jahn–Teller distortions, whereas those at the Mn L_{II} (∼653 eV) edge are primarily associated with direct Goodenough orbital ordering. The middle panel of figure 6 shows the ratio between the integrated intensity at the L_{III} and L_{II} edges. This can provide a measure of the ratio between Jahn–Teller distortions and Goodenough orbital order. Upon warming from the base temperature of these measurements, there is no appreciable change in the ratio of the Jahn–Teller and orbital order, despite the decrease in the AFM order as measured on the $(\frac{1}{4}, \frac{1}{4}, \frac{1}{2})$ reflection. However, at 120 K there is a large discontinuous change corresponding to T_N. As the temperature is increased above T_N, for approximately 20 K, the ratio is observed to decrease asymptotically.

The dramatic decrease in the intensity of the orbital ordering reflection at T_N is very unexpected. This suggests that it is not until T_N that the orbital ordering has fully developed. The fact that T_N also corresponds to the maximum in the branching ratio, suggested that at this temperature, the Jahn–Teller distortions are most dominant in the mechanism of the

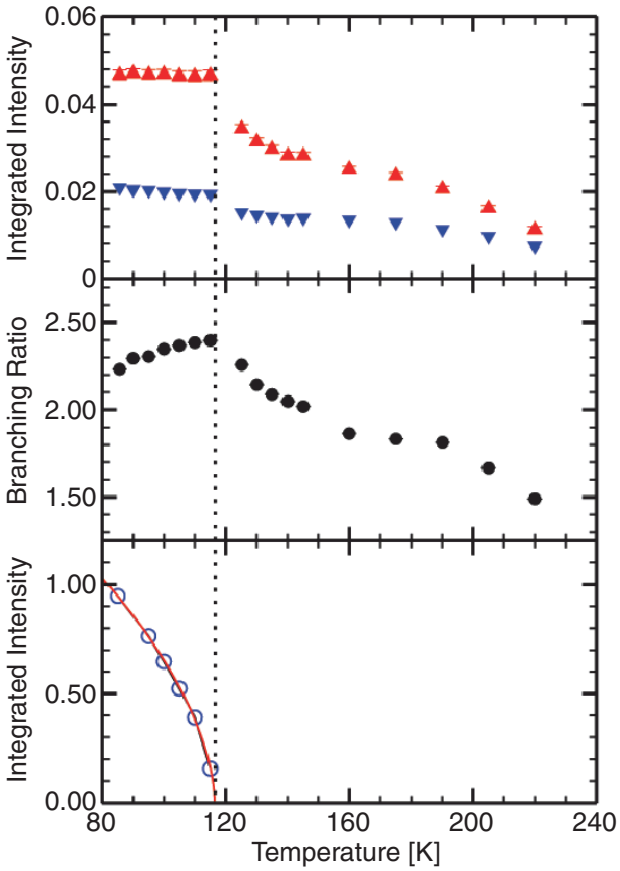

Figure 6. (a) Integrated intensity as a function of temperature of the orbital order superlattice reflection at 641 eV (triangles) and 653 eV (inverted triangles). (b) Ratio of the integrated intensity of the orbital order superlattice reflection as a function of temperature (L_{III}/L_{II}). (c) Integrated intensity of the antiferromagnetic superlattice reflection as a function of temperature. The solid line is a fit to a power law. The fitting errors are within the symbol size.

orbital ordering, compared to direct Goodenough orbital ordering. Below T_N, both the direct Goodenough and the Jahn–Teller components to the orbital order are constant within error. In comparison, the magnetic correlations do increase significantly with decreasing temperature below T_N. Is such behaviour typical, or special just to $La_{0.5}Sr_{1.5}MnO_4$? Because this is one of the first studies to directly measure orbital and magnetic correlations in any material, it is difficult to be certain. However, there are intriguing results obtained by resonant x-ray studies at the K-absorption edge that such effects may be a general feature of strongly correlated 3d transition metal compounds. Such results have not directly probed the 3d band. Rather, as discussed above, K-edge studies probe the 4p band and hence we need to infer, in a rather indirect way, that changes in the 4p band may reflect changes to the 3d band caused by orbital interactions. In $LaMnO_3$, RXS studies at the Mn K edge observed scattering at a wavevector of (1, 0, 0) around allowed Bragg positions. Intensity measurements showed that this scattering, indirectly associated with orbital ordering via Jahn–Teller distortions of the crystal structure, increased dramatically at T_{OO} (∼780 K) and thereafter remained almost constant until just above T_N (∼140 K).

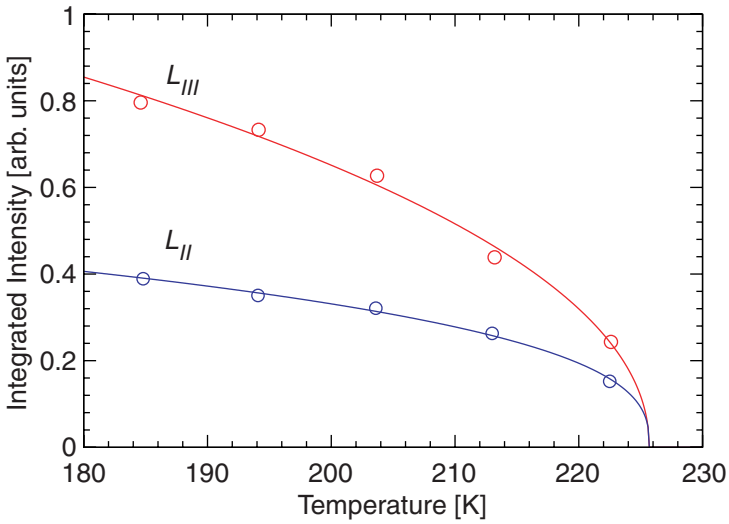

Figure 7. Integrated intensity as a function of temperature of the $(\frac{1}{4}, \frac{1}{4}, 0)$ superlattice reflection at both the Mn L_{III} (∼643 eV) and Mn L_{II} (∼653 eV) edges. The critical exponents for the fits are found to be $\beta = 0.23 \pm 0.01$ and 0.17 ± 0.01 for the L_{III} and L_{II} edges respectively. The fitting errors are smaller than the symbol size.

Just above T_N, the intensity increased by ∼50% and remained constant between T_N and the base temperature [29]. In $KCuF_3$ a doubling in the intensity of the (331) orbital order reflection was observed just above T_N (∼38 K), and again remained constant below T_N [30]. This is similar to $La_{0.5}Sr_{1.5}MnO_4$, where we observe a doubling of the $(\frac{1}{4}, \frac{1}{4}, 0)$ orbital reflection just above T_N. Ishihara and Maekawa [31] suggested that such anomalous changes in the intensity of the orbital order reflection may signal a change in the type of orbital order near the magnetic transition. However, the resonant soft x-ray energy scans are very sensitive to the type of orbital order, as demonstrated by the theoretical calculations of Castleton and Altarelli [25]. Energy scans taken above and below T_N show no dramatic changes to suggest any such change. Rather there is a continuous change in intensity and spectral weight.

Cooling the bilayer manganite $La_{2-2x}Sr_{1+2x}Mn_2O_7$, $x = 0.475$, below T_N caused a marked decrease in the intensity in the Jahn–Teller distorted reflections [32]. This is believed to be caused by the formation of ferromagnetic ordering within the a–b plane, which leads to the disruption of long-range charge and Jahn–Teller distortions. This is exactly opposite to what occurs in $La_{0.5}Sr_{1.5}MnO_4$, where a dramatic increase in the contribution of the cooperative Jahn–Teller distortions to the observed orbital ordering is observed. However, in $La_{0.5}Sr_{1.5}MnO_4$, antiferromagnetic ordering is imposed below T_N which, in tandem with the cooperative Jahn–Teller distortions, strengthens the long-range orbital ordering. Thus the difference in behaviour is a sign of the different magnetic structures formed at low temperatures. Our results therefore reconcile the very different orbital–magnetic interactions in these manganites.

Finally, we consider the second-order transition at T_{OO} ($= T_{CO} \sim 240$ K). Figure 7 displays the intensity of the $(\frac{1}{4}, \frac{1}{4}, 0)$ orbital reflection at the Mn L_{III} (primarily caused by Jahn–Teller distortions) and Mn L_{II} (primarily caused by direct Goodenough orbital order) in the vicinity of T_{OO}. The solid lines are a fit to a power law, where $I = I_0(1 - \frac{T}{T_0})^{2\beta}$ [33]. Below T_{OO}, the

order parameters of the two separable causes of orbital ordering are very different. This shows that at T_{OO}, the Goodenough orbital order mechanism has the largest relative contribution at any temperature. The beta value of the cooperative Jahn–Teller distortions is consistent with the two-dimensional nature within the *a*–*b* plane of the orbital ordering. The lower value of beta for the direct Goodenough orbital order shows that these effects are derived from the cooperative Jahn–Teller distortions. Our results suggest that the cooperative Jahn–Teller distortions are the root cause of the transitions into the charge and orbitally ordered state. Once this is formed, short-range antiferromagnetic correlations occur which further strengthen the long-range orbital ordering (direct Goodenough orbital order). Long-range antiferromagnetism is not realized until much lower temperatures and is accompanied by another increase in the intensity of the orbital ordering.

4. Conclusion

In conclusion, soft x-ray resonant diffraction has been used to directly observe the formation and development of orbital order and magnetic correlations in a half-doped manganite. Our studies have revealed that the two major causes of orbital ordering are Jahn–Teller distortions and short-range antiferromagnetic spin correlations. In addition, we have observed a strong increase in the orbital ordering at the Néel temperature. We believe that this reveals a strong interaction between orbital and magnetic correlations, which may be a general property of many 3d transition metal compounds.

The measurement of the azimuthal dependence of the $(\frac{1}{4}, \frac{1}{4}, 0)$ peak signifies a maturity of the soft x-ray diffraction technique. Successful development of polarization analysis will propel scattering in this energy regime into a mainstream tool.

Acknowledgments

SBW would like to thank the European Commission for support in the frame of the 'Training and Mobility of Researchers' programme. PDH would like to acknowledge support from the University of Durham Research Foundation. We are grateful for support from EPSRC for a studentship for TAWB and CCLRC for access to the SRS and European Synchrotron Radiation Facility (ESRF).

References

[1] Tokure Y and Nagaosa N 2000 *Science* **288** 462
[2] Radaelli P G, Cox D E, Marezio M and Cheong S-W 1997 *Phys. Rev.* B **55** 3015–23
[3] Mutou T and Kontani H 1999 *Phys. Rev. Lett.* **83** 3685–88
[4] Khomskii D and van den Brink J 2000 *Phys. Rev. Lett.* **85** 3329
[5] Hotta T, Dagotto E, Koizumi H and Takada Y 2001 *Phys. Rev. Lett.* **86** 2478
[6] Daoud-Aladine A, Rodriguez-Carvajal J, Pinsard-Gaudart L, Fernandez-Diaz M T and Revcolevschi A 2002 *Phys. Rev. Lett.* **89** 097205
[7] Moritomo Y, Tomioka Y, Asamitsu A, Tokura Y and Matsui Y 1995 *Phys. Rev.* B **51** 3297–3300
[8] Sternlieb B J, Hill J P, Wildgruber U C, Luke G M, Nachumi B, Moritomo Y and Tokura Y 1996 *Phys. Rev. Lett.* **76** 2169–72
[9] Goodenough J B 1955 *Phys. Rev.* **100** 564

[10] Wollan E O and Koehler W C 1955 *Phys. Rev.* **100** 545
[11] Gibbs D, Harshman D R, Isaacs E D, McWhan D B, Mills D and Vettier C 1988 *Phys. Rev. Lett.* **61** 1241–44
[12] Hill J P and McMorrow D F 1996 *Acta Crystallogr.* A **52** 236
[13] Blume M 1985 *J. Appl. Phys.* **57** 3615–8
[14] Blume M and Gibbs D 1988 *Phys. Rev.* B **37** 1779–89
[15] Murakami Y, Kawada H, Kawata H, Tanaka M, Arima T, Moritomo Y and Tokura Y 1998 *Phys. Rev. Lett.* **80** 1932–5
[16] Mizokawa T and Fujimori A 1997 *Phys. Rev.* B **56** R493–R496
[17] Elfimov I S, Anisimov V I and Sawatzky G A 1999 *Phys. Rev. Lett.* **82** 4264–7
[18] Benfatto M, Joly Y and Natoli C R 1999 *Phys. Rev. Lett.* **83** 636–9
[19] Solovyev I V and Terakura K 1999 *Phys. Rev. Lett.* **83** 2825–8
[20] Larochelle S, Mehta A, Kaneko N, Mang P K, Panchula A F, Zhou L, Arthur J and Greven M 2001 *Phys. Rev. Lett.* **87** 095502
[21] Mahadevan P, Terakura K and Sarma D D 2001 *Phys. Rev. Lett.* **87** 066404
[22] Benedetti P, van den Brink J, Pavarini E, Vigliante A and Wochner P 2001 *Phys. Rev.* B **63** 060408
[23] Wilkins S B, Hatton P D, Roper M D, Prabhakaran D and Boothroyd A T 2003 *Phys. Rev. Lett.* **90** 187201
[24] Wilkins S B, Spencer P D, Hatton P D, Collins S P, Roper M D, Prabhakaran D and Boothroyd A T 2003 *Phys. Rev. Lett.* **91** 167205
[25] Castleton C W M and Altarelli M 2000 *Phys. Rev.* B **62** 1033–8
[26] Dhesi S S *et al* 2004 *Phys. Rev. Lett.* **92** 056403
[27] Wilkins S B, Stojic N, Beale T A W, Binggeli N, Castleton C W M, Bencok P, Prabhakaran D, Boothroyd A T, Hatton P D and Altarelli M 2004 *Cond. mat. preprint server* Strongly Correlated Electrons 0410713
[28] Paixao J A, Detlefs C, Longfield M J, Caciuffo R, Santini P, Bernhoeft N, Rebizant J and Lander G H 2002 *Phys. Rev. Lett.* **89** 187202
[29] Murakami Y, Hill J P, Gibbs D, Blume M, Koyama I, Tanaka M, Kawata H, Arima T, Tokura Y, Hirota K and Endoh Y 1998 *Phys. Rev. Lett.* **81** 582–5
[30] Paolasini L, Caciuffo R, Sollier A, Ghigna P and Altarelli M 2002 *Phys. Rev. Lett.* **88** 106403
[31] Ishihara S and Maekawa S 2000 *Phys. Rev.* B **62** R9252–R9255
[32] Wilkins S B, Spencer P D, Beale T A W, Hatton P D, Zimmermann M V, Brown S D, Prabhakaran D and Boothroyd A T 2003 *Phys. Rev.* B **67** 205110
[33] Fujimoto M 1997 *The Physics of Structural Phase Transitions* (Berlin: Springer)